Cyclometalated iridium bipyridine complexes with peripheral antimony substituents

Ying-Hao Lo and Francois P. Gabbai*[a]

Dedicated to Professor Manfred Scheer on the occasion of his 65th birthday

Abstract: As part of our ongoing efforts in the development of main group Lewis acids as anion receptors, we have investigated the synthesis of cyclometalated bipyridine iridium(III) complex decorated by antimony moieties. Reaction of 4-(diphenylstibino)-2,2'-bipyridine (L) with $[(ppy)_2 Ir(\mu\text{-CI})]_2$ afforded the corresponding tris-chelate iridium complex [(ppy)2|rL]+ ([1]+) which was isolated as a hexafluorophosphate salt ([1][PF₆]). Reaction of [1][PF₆] with excess PhICl₂ in DMSO induced the conversion of the diphenvlantimony moiety of [1]+ into an anionic diphenyltrichloroantimonate leading to a zwitterionic complex referred to as 2-Cl. Complexes [1][PF6] and 2-CI have been characterized by NMR and the structure of 2-CI confirmed using X-ray diffraction. DFT calculations and electrochemical measurments show that the electron-rich diphenyltrichloroantimonate moiety in 2-Cl cathodically shifts the Ir(III/IV) redox couple. Luminescence measurements also show that 2-CI is less emissive than [1]+.

The chemistry of organoantimony(V) compounds is experiencing a resurgence that has led to the development of new applications in the area of catalysis,[1] small molecule activation,[2] anion sensing,[3] and anion transport.[4] The most important characteristic of these compounds is the Lewis acidity of the antimony center which can be adjusted by varying the electronic properties of the substituents. These substituents can also be used to impart specific optoelectronic properties which could in principle become useful in the domain of anion sensing. Based on the anion binding reactions shown in Scheme 1, we have shown that appending simple chromophores as in A-C can afford fluorescent turn-on sensors that we have used for the detection of fluoride or cyanide anions at low concentrations (Figure 1). $^{[3a,\ 3b,\ 3e]}$ We have also considered the use of metal containing chromophores as in the case **D**, a complex in which the tetraaryl stibonium cation is installed at the periphery of a cyclometalated ruthenium polypyridyl core (Figure 1). [5] Our investigation of the properties of this complex showed that anion coordination at the antimony centers triggers electrochemical and photophysical changes that can be used to report the chemistry taking place at the Lewis acidic main group center. Building on these recent results, we have now become

Y.-H Lo and F. P. Gabbaï Department of Chemistry, Texas A&M University College Station, TX 77843 (USA) E-mail: francois@tamu.edu

Homepage: http://www.chem.tamu.edu/rgroup/gabbai/ Supporting information for this article is given via a link at the end of

the document.

interested in installing antimony(V) moieties at the periphery of other metal complexes.

Scheme 1: Anion binding reaction involving antimony(V) species (X = halogen).

Figure 1. Structure of relevant antimony(V) Lewis acids and general structure targeted in this study.

Iridium (III) cyclometalated complexes constitute an important class of materials that have found applications in sensing, photocatalysis, and light emitting or harvesting materials. [6] The most important property of these complexes is the metal-to-ligand charge transfer (MLCT) nature of their excited state as it influences the emissive properties of these materials as well as their photoredox properties. Because of the attractive features displayed by iridium (III) cyclometalated complexes, we have now become interested in investigating the incorporation of Lewis acidic antimony moieties at their periphery. In this paper, we describe a series of results obtained while pursuing this objective.

Results and Discussion

We have previously described 4-(diphenylstibino)-2,2'-bipyridine (L), a ligand that we successfully incorporated in platinum(II)

complexes.^[7] We found that this ligand reacted cleanly with $[(ppy)_2|r(\mu-Cl)]_2$ (ppy = 2-phenylpyridine) in refluxing methanol and dichloromethane (1:1 v/v) to afford, after anion exchange with KPF₆, the antimony-substituted iridium complex [1][PF₆] as a yellow solid (Scheme 2).^[8] This complex was subsequently allowed to react with excess phenyl iodine dichloride (PhICl₂) in wet DMSO to afford complex **2**-Cl which also displays a yellow color characteristic of the iridium tris-chelate chromophore. Dissolution of PhICl₂ in DMSO is exothermic, suggesting oxidation of DMSO,^[9] which in the presence of water would release HCl and the resulting sulfone. We propose that this side reaction is the source of the third chloride anion coordinated to the antimony atom. We also attempted to oxidize [1][PF₆] with o-chloranil, which resulted in a mixture of products which we have not yet been able to identify.

Scheme 2. Synthesis of [1][PF $_6$] and 2-Cl.(a) 1 equiv. [(ppy) $_2$ Ir($_4$ Cl)] $_2$, DCM/MeOH 1:1, reflux, 8 h. (b) KPF $_6$, MeOH (c) 4 equiv. PhICl $_2$, DMSO, 3 h. (d) 1 equiv. AgOTf, CDCl $_3$.

Both [1][PF₆] and 2-Cl have been fully characterized by ¹H and ¹³C NMR spectroscopy. The ¹H NMR spectra of [1][PF₆] and 2-Cl display complicated spectra because the symmetry of the pseudo-octahedral iridium complex is broken by the coordination of the L, making each aromatic hydrogen magnetically nonequivalent. It is worth noting that the diagnostic peaks corresponding to the 3 position of the bipyridine ligand shifts from 8.63 ppm to 9.24 ppm upon oxidation. The resonances corresponding to the phenyl group bound to the antimony atom also display a significant shift from 7.35 ppm to 7.68 ppm, indicative of a more electrophilic environment as a result of antimony oxidation (Figure 2). The ESI mass spectrum of 2-CI is dominated by a peak at m/z 1001 amu corresponding to [2]+ (Scheme 2) with an isotopic pattern consistent with the atomic make up of this cation. The detection of this complex suggests that 2-Cl could release a chloride anion to afford the corresponding iridium-stiborane [2]+. To test this possibility, 2-Cl was suspended in CDCl₃, a solvent in which it is not soluble. Addition of AgOTf to this mixture resulted in dissolution of the complex and the appearance of ¹H NMR resonances assigned to the formation of [2][OTf] which could unfortunately not be isolated.

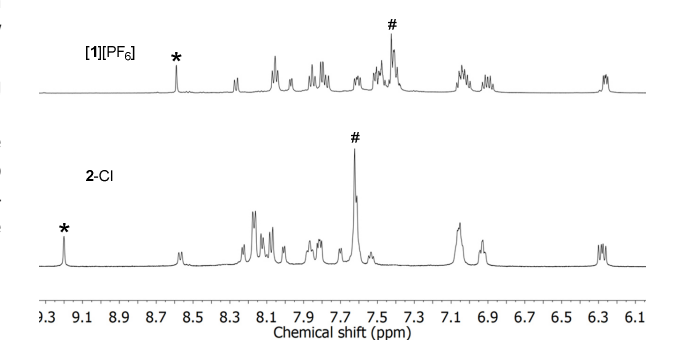


Figure 2. ¹H NMR spectra of complexes [1][PF₆] and **2**-Cl in CD₃CN. The proton ortho to the cyclometalating carbon is indicated by an asterisk (*) for each spectrum. The protons corresponding to the phenyl group on the antimony are indicated by a pound sing (#).

The solid-state structure of complex **2**-Cl has been determined using single crystal X-ray diffraction analysis (Figure 3). The iridium (III) center adopts a distorted octahedral geometry, with the N(1)-Ir(1)-N(2) bond angle compressed to 76.2(3)°, a feature consistent with literature precedents for these type of complexes. [10] A comparison of the structure of **2**-Cl with that of [Ir(ppy)₂(bpy)]⁺ shows that the antimony moiety has negligible influence on the geometry of the iridium center. [11] The antimony center also displays a distorted octahedral geometry with the three chloride ligands in a *mer*-configuration. The longer Sb(1)-Cl(3) distance (2.547(2) Å), compared to Sb(1)-Cl(1) and Sb(1)-Cl(2) (2.370(5) Å and 2.472(3) Å) suggests that the pyridyl ring at the trans position exerts a greater trans influence than that of a chlorine ligand.

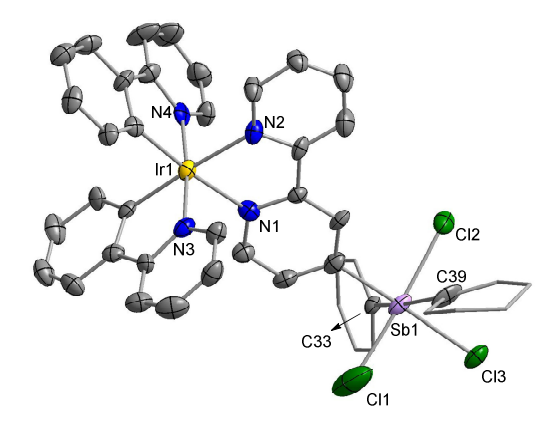


Figure 3. Solid-state structure of 2-CI. Thermal ellipsoids are drawn at the 50% probability level. The hydrogen atoms are omitted for clarity. Selected bond length (Å) and angles (deg):

Sb1-Cl1 2.370(5), Sb-Cl2 2.472(3), 2.547(2), N1-Ir1-N2 76.2(3).

The photophysical properties of [1][PF₆] and 2-Cl have been studied and compared with those of the parent complex [(ppy)₂lr(bpy)][PF₆] for reference. The absorption spectrum of the two new iridium complexes and that of the reference are shown in Figure 4. The low energy absorption bands of all three complexes display a similar profile. The absorption features at 350 nm - 450 nm are assigned to the ligand-to-ligand charge transfer (ppy to bpy, 1LLCT) and metal-to-ligand charge transfer processes (iridium to ppy or bpy, ¹MLCT).^[12] In addition, the very weak absorptions between 450 to 470 nm were assigned to ³LLCT and ³MLCT. The similarity of these three spectra indicates that the antimony moiety, oxidized or not, has negligible effects on the energy of these transitions. This may at first surprising, especially in the case of the oxidized complex 2-Cl. We speculate that formation of the trichloroantimonate moiety somewhat counters the increased electron-withdrawing properties of the oxidized antimony center.

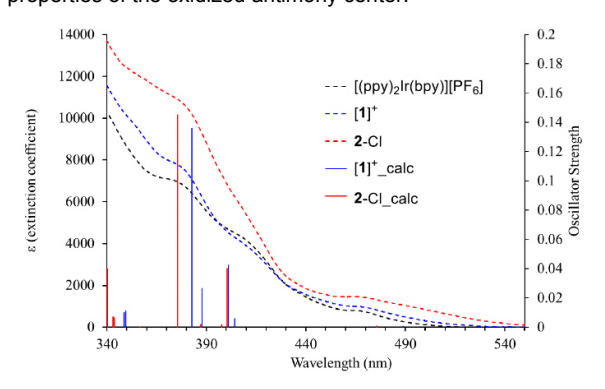


Figure 4. Experimental UV-vis spectra of [1][PF $_6$], **2**-Cl and [(ppy) $_2$ lr(bpy)][PF $_6$] in acetonitrile at room temperature. Experimental UV-vis spectrum and calculated vertical electronic transitions (represented by bars) for [1][PF $_6$] and **2**-Cl in acetonitrile. The wavelengths of the calculated transitions are plotted against the oscillator strengths.

We have also computed the electronic structure of [1]+ and 2-Cl using density functional theory (DFT). These calculations were carried out using the Gaussian program with B3LYP as a functional and a mixed basis set (Sb/Ir cc-pVTZ-PP; C/H/N/Cl 3/21G*).[13] The optimized structures are in reasonable agreement with those measured using X-ray diffraction (see the Supporting Information). Figure 5 displays the contours and energies of the Kohn-Sham highest occupied molecular orbital (HOMO) and lowest occupied molecular orbital (LUMO). In both [1] and 2-Cl. the HOMO and LUMO are dominated by an iridium " t_{2q} " orbital and the bipyridine π^* orbital, respectively. These frontier orbitals closely resemble those of [(ppy)₂lr(bpy)]⁺.^[6c] An interesting feature in the case of 2-Cl is the contribution of a chloride p-orbital to the HOMO of the complex, consistent with the electron rich nature of the antimonate anion. There is a notable change in the HOMO-LUMO gap which increases from 2.8 ev in [1]+ to 3.26 ev in 2-Cl. This relatively large difference appears difficult to reconcilliate with the experimental

spectroscopic results which show similar UV-vis absorption profiles for both [1]+ and 2-Cl. To shed light on this apparent discrepancy, we resorted to TD-DFT calculations using the solute electron density-based implicit solvation model (SMD) with acetonitrile as a solvent. The results of these calculations afford a series of intense vertical excitations, the energy of which nicely coincides with the main absorption features observed in the experimental spectra (Figure 4). There are also a series of weaker transitions, some of which appear in the lower energy range of the spectrum. To better understand the character of these vertical excitations, each of them were analyzed using the natural transition orbital (NTO) method. The results of this analysis show that, for both complexes, the HOMO-LUMO transition has almost inexistent oscillator strength (f = 0.001). This simple computational indicates that the HOMO-LUMO transition does not contribute to the absorption spectrum of these derivatives which are, as a result, not affected by the respective energy of these two orbitals. The NTO analysis of the TD-DFT results shows that the first vertical excitation of respectable oscillator strength (f > 0.04) have HOMO to LUMO+1 character for [1]+ and HOMO to LUMO+2 for 2-Cl (Table 1). These excitations correspond to the third and second excited states in the case of [1]+ and 2-Cl, respectively. It is interesting to note the LUMO+1 for [1]+ and LUMO+2 for 2-Cl are π^* orbitals delocalized on the phenylpyridine ligands rather than on the bipyridine ligand. Moreover, the energy of this transition $(401.1 \text{ nm for } [1]^+ \text{ with } f = 0.04 \text{ and } 400.4 \text{ nm for } 2\text{-Cl with } f = 0.04 \text{ mm}$ 0.04) is almost identical in both compounds, thereby providing a rationale for the similarity of the spectra of these two compounds. The next intense vertical excitation, which are calculated at 382.7 nm for $[1]^+$ (f = 0.14) and 375.5 nm for 2-Cl (f = 0.15), correspond to the fifth singlet excited state for both complexes. The NTO analysis shows that this transition involves excitation from an orbital of HOMO-1/HOMO-2 character to the LUMO which as stated above has bipyridine π^* character. Again, the similarity in the energy of these transitions in the two complexes explains why their UV-vis spectra are so alike.

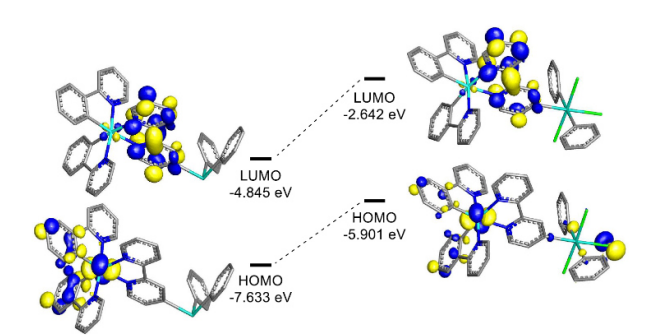
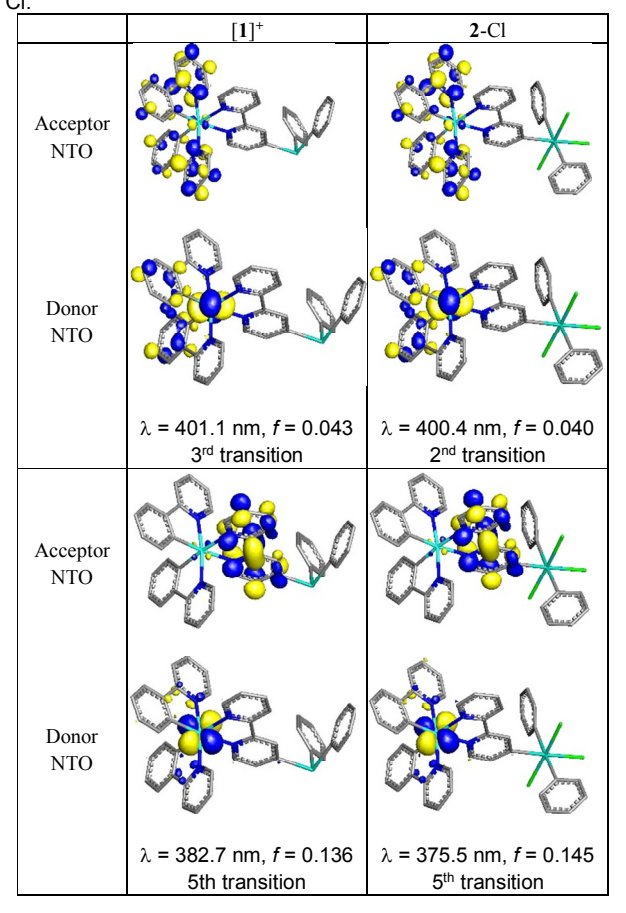


Figure 5. Frontier molecular orbitals (isovalue 0.05) and Energies (eV) of [1]+ and 2-Cl.

Table 1. Dominant NTOs, calculated wavelengths (λ), and oscillator strengths (f) for the excited singlet states of [1]⁺ and 2-



The emission spectra of complex [(ppy)₂lr(bpy)][PF₆], [1][PF₆] and **2**-Cl in acetonitrile are shown in Figure 6. Similar to the absorption spectrum, the emission maxima (λ_{em} = 595 nm) and quantum yield of [1][PF₆] (Φ = 9.3%) show almost no differences when compared to [(ppy)₂lr(bpy)][PF₆] (λ_{em} = 592 nm, Φ = 9.3%).^[13b] This suggests that the diphenyl antimony substituent has no influence on the iridium-centered fluorophore. Interestingly, a noticeable red shift (25 nm) is observed for the emission of **2**-Cl (λ_{em} = 617 nm) and the quantum yield drops to 2.2%. We propose that the lower quantum yield of **2**-Cl originates from a decrease in the transition dipole moment caused by the presence of the anitmonate moiety.^[14]

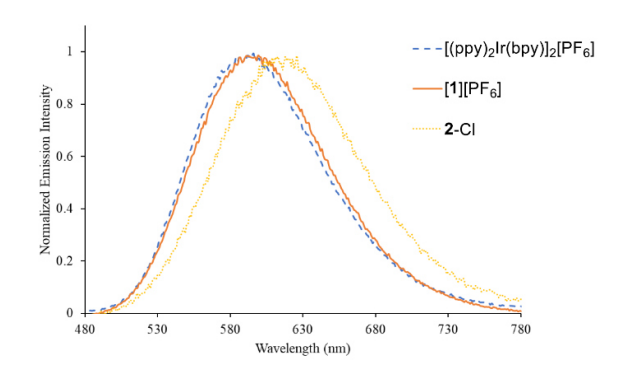


Figure 6. Luminescence spectra of $[(ppy)_2|r(bpy)]^+$, [1]⁺ and **2**-Cl in CH₃CN solution at 298 k. λ_{ex} = 400 nm.

The cyclic voltammograms of [1][PF6] and 2-Cl were recorded and were also compared with that of [(ppy)₂lr(bpy)][PF₆] (Figure 7). Both [1][PF₆] and 2-Cl display a quasi-reversible reduction wave at $E_{1/2}$ = -1.78 V and -1.77 V, respectively, attributed to the reduction of the bipyridine ligand. This reduction is irreversible in the case of 2-Cl, a feature that we correlate to the possible coupling of the electron transfer event to a reduction of the antimony (V) center, mediated by the bipyridine ligand. The voltammograms also display a quasi-reversible wave assigned to the Ir(III)/(IV) couple. This wave is observed 0.89 V for [1]+, which is also close to that of $[(ppy)_2|r(bpy)][PF_6]$ (E_{1/2} = 0.88 V). The small difference in both redox potentials points to the innocence of the diphenylantimony moiety in [1]+. In the case of 2-Cl, the Ir(III/IV) redox couple observed at 0.79 V is shifted cathodically by 80 mV. This shift indicates that iridium center in complex 2-Cl is more electron-rich. This result is consistent with the fact that this complex is neutral and thus more prone to oxidation than cationic [1]+.

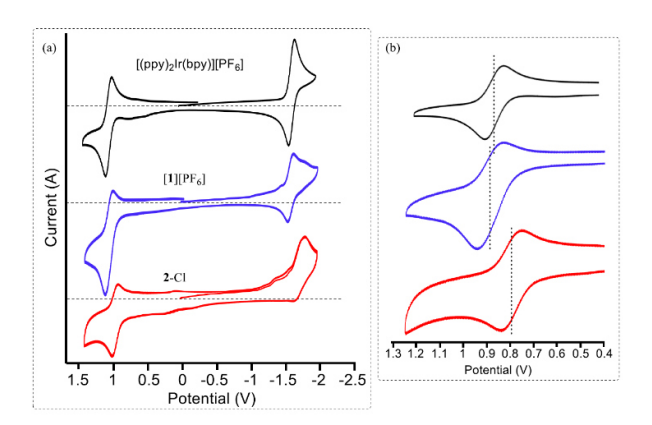


Figure 7. Cyclic voltammograms of [1][PF₆], **2**-Cl and [(ppy)₂lr(bpy)][PF₆] in acetonitrile with 0.1 M ["Bu₄N][PF₆] as electrolyte. The scan rate was 0.1V/s, and potentials are referenced to Fc/Fc⁺ in the same solvent.

Conclusion

In summary, we have synthesized two cyclometalated iridium bipyridine complexes bearing a peripheral Sb(III) or Sb(V) substituent. The similar properties displayed by [1]* and the reference complex [(ppy)₂Ir(bpy)]* suggests that the diphenylantimony group does not interfere with the optoelectronic properties of the iridium complex. Finally, we have also shown that the antimony moiety of [1]* can be oxidized into a stiborane unit which readily binds an extra chloride anion, leading to the formation of a trichloroantimonate moiety as in 2-Cl. Formation of this anionic substituent renders the complex neutral and makes oxidation of the iridium center slightly more facile that in the cationic precursor. Finally, we note that 2-Cl is also notably less emissive that its precursor [1]*.

Experimental Section

All preparations were carried out under an N2 atmosphere using standard Schlenk techniques unless otherwise stated. 4-Bromobipyridine, Ph₂SbCl, [15] [16] PhICl₂, [17] were prepared according to previously reported procedures. Et₂O and THF were dried by refluxing under N₂ over Na/K. CH₃CN was dried over CaH₂. All other solvents were ACS reagent grade and used as received. All chemicals were purchased from Sigma-Aldrich, Merck, or Spectrochem and used as received. Thin-layer chromatography (TLC) was performed on a Merck 60 F254 silica gel plate (0.25 mm thickness). Column chromatography was performed on a Merck 60 silica gel (100-200 mesh). Ambient temperature NMR spectra were recorded on a Varian Unity Inova 500 FT NMR (499.42 MHz for ¹H, 125.58 MHz for ^{13}C) spectrometer. Chemical shifts (δ) are given in ppm and are referenced against the solvent signals (1H, 13C). Elemental analyses were performed at Atlantic Microlab (Norcross, GA). Absorbance measurements were taken on a Shimadzu UV-2502PC UV-Vis spectrophotometer against a solvent reference.

Crystallography. All crystallographic measurements were performed at 110(2) K using a Bruker SMART APEX II diffractometer with a CCD area detector (graphite monochromated Mo Kα radiation, λ = 0.71073 Å, ωscans with a 0.5° step in ω). In each case, a specimen of suitable size and quality was selected and mounted onto a nylon loop. The semiempirical method SADABS^[18] was applied for absorption correction. The structures were solved by direct methods and refined by the full-matrix least-squares technique against F^2 with anisotropic temperature parameters for all non-hydrogen atoms. All H atoms were geometrically placed and refined using the riding model approximation. Data reduction and further calculations were performed using the Bruker Apex2 (2013) and SHELXTL^[19] program packages. Structural refinements were performed using Olex2.^[20]

Computational details. Density functional theory (DFT) structural optimizations were conducted using the Gaussian 09 program. [21] In all cases, the structures were optimized using the B3LYP[22] functional. In order to optimize the efficiency of our computations while still treating the heavy atoms at a sufficient level of theory, we used the following mixed basis set: Sb/Ir, cc-pVTZ-PP; C/H/N, 6-31g; Cl, 3-21g(d') with effective core potentials for the heavy elements. [23] Optimizations with the MPW1PW91 functional and the same basis sets were considered but abandoned because they afforded geometries exhibiting large deviations from the experimental ones. For all optimized structures, frequency calculations were carried out to confirm the absence of imaginary frequencies. TD-DFT calculations were carried out using the B3LYP

functional and the SMD solvation model. The molecular orbitals were visualized and plotted using the Jimp2 program.^[24]

Electrochemistry. Electrochemical experiments were performed with an electrochemical analyzer from CH Instruments (model 610A) with a glassy-carbon working electrode and a platinum auxiliary electrode. The reference electrode was built from a silver wire inserted into a small glass tube fitted with a porous Vycor frit at the tip and filled with a THF solution containing tetrabutylammonium hexafluorophosphate (TBAPF6, 0.1 M) and AgNO3 (0.005 M). All three electrodes were immersed in a deoxygenated DMF solution (5 mL) containing TBAPF6 (0.1 M) as a support electrolyte and platinum complexes ([1][PF6], 2-Cl and [(ppy)2lr(bpy)][PF6] (0.001 M). Ferrocene was used as an internal standard, and all potentials are reported with respect to E1/2 of the Fc / Fc+ redox couple.

Synthesis of [1][PF₆]. The ligand L (150 mg, 0.35 mmol) and [(ppy)₂lr(μ -Cl)]2 (187 mg, 0.17 mmol) were combined in a methanol and dichloromethane mixture (1:1 v/v). The resulting suspension was stirred for 8 h under reflux. The solution was concentrated, and treated with KPF₆ (200 mg, 1.1 mmol). The precipitate was isolated by filtration and washed with water (3 × 5 mL), Et₂O (3 × 3 mL), and dried under vacuum to give a [1][PF $_6$] as a yellow solid. Yield: 309 mg (83%). 1H NMR (499.42 MHz, (CD₃CN) δ 8.59 (s, 1H), 8.27 (d, J = 8.1 Hz, 1H), 8.08 – 8.03 (m, 4H), 7.97 (d, J = 5.5 Hz, 1H), 7.85 (t, J = 7.8 Hz, 2H), 7.82 – 7.76 (m, 3H), 7.61 (dd, J = 9.8, 5.8 Hz, 2H), 7.54 – 7.46 (m, 4H), 7.45 – 7.37 (m, 6H), 7.09 - 6.99 (m, 5H), 6.94 - 6.86 (m, 2H), 6.28 - 6.23 (m, 2H). ¹³C NMR (125.58 MHz, CD₃CN) δ 168.32, 168.29, 156.66, 156.08, 155.41, 151.58, 151.45, 151.15, 150.16, 150.13, 150.04, 144.97, 144.94, 140.20, 139.47, 139.45, 138.15, 137.25, 137.19, 135.89, 132.43, 132.42, 131.30, 131.26, 130.41, 130.40, 130.31, 130.29, 129.24, 125.82, 125.77, 125.40, 124.44, 123.47, 123.44, 120.80. Elemental analysis (%) calculated for C₄₄H₃₃F₆IrN₄PSb: C, 49.08; H, 3.09. Found: C, 49.18; H, 3.17.

Synthesis of 2-CI. Complex [1][PF6] (100 mg, 0.09 mmol) was dissolved in DMSO (5mL) and treated with PhICl₂ (99 mg, 0.36 mmol) in DMSO (1 mL). The resulting yellow solution was stirred for 1 hour. The solution was extracted with pentane (3× 3 mL) to remove Phl. Next the DMSO solution was treated with portions of diethyl ether (3 × 3 mL). After each addition of diethyl ether, the top layer was removed and discarded, leading to an effective concentration of the bottom DMSO layer. The resulting DMSO solution was treated with dichloromethane (1 mL) and diethyl ether (10 mL) leading to the formation of an orange solid precipitate identified as 2-Cl. Yield: 69 mg (74%). Single crystals of 2-Cl suitable for X-ray diffraction were obtained by diffusion of diethyl ether in to a solution of the compound in acetonitrile. ¹H NMR (499.42 MHz, CD₃CN) δ 9.20 (s, 1H), 8.60 (d, J = 8.2 Hz, 1H), 8.26 (d, J = 5.6 Hz, 1H), 8.20 (m, 4H), 8.14 (m,2H), 8.08 (d, J = 8.3 Hz, 2H), 8.02 (d, J = 5.4 Hz, 1H), 7.90 (m, 2H), 7.82 (d, J = 7.9 Hz, 2H), 7.70 (d, J = 5.7 Hz, 1H), 7.65 (m, 7H), 7.55 (dd, J = 7.5, 5.6 Hz, 1H), 7.06 (m, 4H), 6.93 (t, J = 7.4 Hz,2H), 6.28 (dd, J = 12.3, 7.5 Hz, 2H). ¹³C NMR (126 MHz, CD₃CN) δ 168.26, 168.18, 157.12, 156.06, 151.83, 151.60, 150.89, 150.71, 150.44, 150.41, 145.00, 144.90, 143.37, 140.45, 139.66, 139.60, 134.60, 133.88, $133.04,\ 132.46,\ 132.36,\ 131.82,\ 131.37,\ 131.35,\ 130.65,\ 130.03,\ 129.82,$ 128.34, 126.12, 125.86, 124.59, 124.51, 123.67, 123.63, 120.91, 120.88. Elemental analysis (%) calculated for C₄₄H₃₃Cl₃lrN₄Sb: C, 50.91; H, 3.20. Found: C, 50.66; H, 3.74.

Generation of [2][OTf]. To a suspension of **2**-Cl (10 mg, 0.01 mmol) in CDCl₃ (0.5 mL) was added solid AgOTf (2.6 mg, 0.01 mmol). The yellow precipitate of **2**-Cl dissolved upon stirring while a AgCl precipitated as a white powder. The resulting yellow solution of [2][OTf] was analyzed by ¹H NMR spectroscopy. ¹H NMR (499.42 MHz, CDCl₃) δ 9.33 (s, 1H), 8.57 (d, J = 8.0 Hz, 1H), 8.28 (m, 3H), 8.14 (t, J = 7.9 Hz, 1H), 8.11 (d, J = 5.6 Hz, 1H), 7.97 (d, J = 5.3 Hz, 1H), 7.92 (d, J = 8.3 Hz, 2H), 7.78 (t, J

= 7.8 Hz, 2H), 7.69 (t, J = 8.3 Hz, 2H), 7.61 (m, 10H), 7.45 (m, 1H), 7.07 (m, 4H), 6.93 (m, 2H), 6.29 (dd, J = 14.7, 7.6 Hz, 2H).

Acknowledgements

This work was supported by the National Science Foundation (CHE-1856453), the Welch Foundation (A-1423), and Texas A&M University (Arthur E. Martell Chair of Chemistry).

Keywords: antimony • iridium • chloride anion • luminescence • redox reaction

References

- [1] a) S. Benz, A. I. Poblador-Bahamonde, N. Low-Ders, S. Matile, Angew. Chem. Int. Ed. 2018, 57, 5408-5412; b) M. Yang, D. Tofan, C.-H. Chen, K. M. Jack, F. P. Gabbaï, Angew. Chem. Int. Ed. 2018, 57, 13868-13872; c) S. S. Chitnis, H. A. Sparkes, V. T. Annibale, N. E. Pridmore, A. M. Oliver, I. Manners, Angew. Chem. Int. Ed. 2017, 56, 9536-9540; d) M. Yang, N. Pati, G. Belanger-Chabot, M. Hirai, F. P. Gabbaï, Dalton Trans. 2018, 47, 11843-11850; e) A. Baba, M. Fujiwara, H. Matsuda, Tetrahedron Lett. 1986, 27, 77-80; f) M. Fujiwara, A. Baba, H. Matsuda, J. Heterocycl. Chem. 1988, 25, 1351-1357; g) R. Arias-Ugarte, D. Devarajan, R. M. Mushinski, T. W. Hudnall, Dalton Trans. 2016, 45, 11150-11161; h) R. Arias-Ugarte, T. W. Hudnall, Green Chemistry 2017, 19, 1990-1998; i) N. Li, R. Qiu, X. Zhang, Y. Chen, S.-F. Yin, X. Xu, Tetrahedron 2015, 71, 4275-4281; j) M. Hirai, J. Cho, F. P. Gabbaï, Chem. Eur. J. 2016, 22, 6537-6541; k) B. Pan, F. P. Gabbaï, J. Am. Chem. Soc. 2014, 136, 9564-9567; l) M. Yang, F. P. Gabbaï, Inorg. Chem. 2017, 56, 8644-8650.
- [2] a) D. Tofan, F. P. Gabbaï, *Chem. Sci.* **2016**, *7*, 6768-6778; b) G. K. Fukin, E. V. Baranov, A. I. Poddel'sky, V. K. Cherkasov, G. A. Abakumov, *ChemPhysChem* **2012**, *13*, 3773-3776; c) A. I. Poddel'sky, Y. A. Kurskii, A. V. Piskunov, N. V. Somov, V. K. Cherkasov, G. A. Abakumov, *Appl. Organomet. Chem.* **2011**, *25*, 180-189; d) V. K. Cherkasov, G. A. Abakumov, E. V. Grunova, A. I. Poddel'sky, G. K. Fukin, E. V. Baranov, Y. V. Kurskii, L. G. Abakumova, *Chem. Eur. J.* **2006**, *12*, 3916-3927.
- [3] a) I.-S. Ke, M. Myahkostupov, F. N. Castellano, F. P. Gabbaï, *J. Am. Chem. Soc.* **2012**, *134*, 15309-15311; b) M. Hirai, F. P. Gabbaï, *Chem. Sci.* **2014**, *5*, 1886-1893; c) M. Hirai, F. P. Gabbaï, *Angew. Chem. Int. Ed.* **2015**, *54*, 1205-1209; d) M. Hirai, M. Myahkostupov, F. N. Castellano, F. P. Gabbaï, *Organometallics* **2016**, *35*, 1854-1860; e) A. M. Christianson, F. P. Gabbaï, *Chem. Commun.* **2017**, *53*, 2471-2474; f) A. Kumar, M. Yang, M. Kim, F. P. Gabbaï, M. H. Lee, *Organometallics* **2017**, *36*, 4901-4907; g) A. M. Christianson, F. P. Gabbaï, *Organometallics* **2017**, *36*, 3013-3015; h) A. M. Christianson, E. Rivard, F. P. Gabbaï, *Organometallics* **2017**, *36*, 2670-2676; i) J. Qiu, B. Song, X. Li, A. F. Cozzolino, *PCCP* **2018**, *20*, 46-50.
- [4] a) L. M. Lee, M. Tsemperouli, A. I. Poblador-Bahamonde, S. Benz, N. Sakai, K. Sugihara, S. Matile, J. Am. Chem. Soc. 2019, 141, 810-814; b) G. Park, D. J. Brock, J.-P. Pellois, F. P. Gabbaï, Chem 2019.
- [5] A. M. Christianson, F. P. Gabbaï, J. Organomet. Chem. 2017, 847, 154-161.
- [6] a) J. Twilton, C. Le, P. Zhang, M. H. Shaw, R. W. Evans, D. W. C. MacMillan, Nature Reviews Chemistry 2017, 1, 0052; b) K. K. Lo, Acc. Chem. Res. 2015, 48, 2985-2995; c) R. D. Costa, E. Ortí, H. J. Bolink, F. Monti, G. Accorsi, N. Armaroli, Angew. Chem. Int. Ed. 2012, 51, 8178-8211; d) I. M. Dixon, J.-P. Collin, J.-P. Sauvage, L. Flamigni, S. Encinas, F. Barigelletti, Chem. Soc. Rev. 2000, 29, 385-391.
- [7] Y.-H. Lo, F. P. Gabbaï, *Organometallics* **2018**, *37*, 2500-2506.
- [8] E. Sauvageot, P. Lafite, E. Duverger, R. Marion, M. Hamel, S. Gaillard, J.-L. Renaud, R. Daniellou, *J. Organomet. Chem.* **2016**, *808*, 122-127.
- [9] G. Barbieri, M. Cinquini, S. Colonna, F. Montanari, *Journal of the Chemical Society C: Organic* **1968**, 659-663.

- [10] a) Ł. Skórka, M. Filapek, L. Zur, J. G. Małecki, W. Pisarski, M. Olejnik, W. Danikiewicz, S. Krompiec, *The Journal of Physical Chemistry C* 2016, 120, 7284-7294; b) T. Mizuno, M. Takeuchi, I. Hamachi, K. Nakashima, S. Shinkai, J. Chem. Soc., Perkin Trans. 2 1998, 2281-2288; c) G. Zhou, C.-L. Ho, W.-Y. Wong, Q. Wang, D. Ma, L. Wang, Z. Lin, T. B. Marder, A. Beeby, *Adv. Funct. Mater.* 2008, 18, 499-511.
- [11] K. R. Schwartz, R. Chitta, J. N. Bohnsack, D. J. Ceckanowicz, P. Miró, C. J. Cramer, K. R. Mann, *Inorg. Chem.* **2012**, *51*, 5082-5094.
- [12] S.-H. Wu, J.-W. Ling, S.-H. Lai, M.-J. Huang, C. H. Cheng, I. C. Chen, The Journal of Physical Chemistry A 2010, 114, 10339-10344.
- [13] a) S. Ladouceur, D. Fortin, E. Zysman-Colman, *Inorg. Chem.* **2011**, *50*, 11514-11526; b) S. Ladouceur, D. Fortin, E. Zysman-Colman, *Inorg. Chem.* **2010**, *49*, 5625-5641.
- [14] C. Dragonetti, L. Falciola, P. Mussini, S. Righetto, D. Roberto, R. Ugo, A. Valore, F. De Angelis, S. Fantacci, A. Sgamellotti, M. Ramon, M. Muccini, *Inorg. Chem.* 2007, 46, 8533-8547.
- [15] B. A. Chalmers, M. Bühl, K. S. Athukorala Arachchige, A. M. Z. Slawin, P. Kilian, Chem. Eur. J. 2015, 21, 7520-7531.
- [16] D. A. M. Egbe, A. M. Amer, E. Klemm, *Designed Monomers and Polymers* **2001**, *4*, 169-175.
- [17] X.-F. Zhao, C. Zhang, Synthesis 2007, 551-557.
- [18] G. M. Sheldrick, Bruker Analytical X-ray Systems Inc., Madison, Wisconsin, USA, 2007.
- [19] G. M. Sheldrick, SHELXTL-2008/2004, Structure Determination Software Suite, Bruker AXS, Madison, Wisconsin, USA, 2008.
- [20] O. V. Dolomanov, L. J. Bourhis, R. J. Gildea, J. A. K. Howard, H. Puschmann, J. Appl. Crystallogr. 2009, 42, 339-341.
- [21] M. J. Frisch, G. W. Trucks, H. B. Schlegel, G. E. Scuseria, M. A. Robb, J. R. Cheeseman, G. Scalmani, V. Barone, B. Mennucci, G. A. Petersson, H. Nakatsuji, M. Caricato, X. Li, H. P. Hratchian, A. F. Izmaylov, J. Bloino, G. Zheng, J. L. Sonnenberg, M. Hada, M. Ehara, K. Toyota, R. Fukuda, J. Hasegawa, M. Ishida, T. Nakajima, Y. Honda, O. Kitao, H. Nakai, T. Vreven, J. Montgomery, J. A.; , J. E. Peralta, F. Ogliaro, M. Bearpark, J. J. Heyd, E. Brothers, K. N. Kudin, V. N. Staroverov, R. Kobayashi, J. Normand, K. Raghavachari, A. Rendel, J. C. Burant, S. S. Iyengar, J. Tomasi, M. Cossi, N. Rega, J. M. Millam, M. Klene, J. E. Knox, J. B. Cross, V. Bakken, C. Adamo, J. Jaramillo, R. Gomperts, R. E. Stratmann, O. Yazyev, A. J. Austin, R. Cammi, C. Pomelli, J. W. Ochterski, R. L. Martin, K. Morokuma, V. G. Zakrzewski, G. A. Voth, P. Salvador, J. J. Dannenberg, S. Dapprich, A. D. Daniels, Ö. Farkas, J. B. Foresman, J. V. Ortiz, J. Cioslowski, D. J. Fox, *Gaussian 09*, Revision B.01, Gaussian, Inc.: Wallingford, CT, **2009**.
- [22] a) A. D. Becke, J. Chem. Phys. 1993, 98, 5648-5652; b) P. J. Stephens,
 F. J. Devlin, C. F. Chabalowski, M. J. Frisch, The Journal of Physical Chemistry 1994, 98, 11623-11627.
- [23] a) M. J. Frisch, G. W. Trucks, H. B. Schlegel, G. E. Scuseria, M. A. Robb, J. R. Cheeseman, G. Scalmani, V. Barone, B. Mennucci, G. A. Petersson, H. Nakatsuji, M. Caricato, X. Li, H. P. Hratchian, A. F. Izmaylov, J. Bloino, G. Zheng, J. L. Sonnenberg, M. Hada, M. Ehara, K. Toyota, R. Fukuda, J. Hasegawa, M. Ishida, T. Nakajima, Y. Honda, O. Kitao, H. Nakai, T. Vreven, J. Montgomery, J. A.; , J. E. Peralta, F. Ogliaro, M. Bearpark, J. J. Heyd, E. Brothers, K. N. Kudin, V. N. Staroverov, R. Kobayashi, J. Normand, K. Raghavachari, A. Rendell, J. C. Burant, S. S. Iyengar, J. Tomasi, M. Cossi, N. Rega, J. M. Millam, M. Klene, J. E. Knox, J. B. Cross, V. Bakken, C. Adamo, J. Jaramillo, R. Gomperts, R. E. Stratmann, O. Yazyev, A. J. Austin, R. Camm, C. Pomelli, J. W. Ochterski, R. L. Martin, K. Morokuma, V. G. Zakrzewski, G. A. Voth, P. Salvador, J. J. Dannenberg, S. Dapprich, A. D. Daniels, Ö. Farkas, J. B. Foresman, J. V. Ortiz, J. Cioslowski, D. J. Fox, *Gaussian 09*, Revision D.01, Gaussian, Inc., Wallingford, CT, **2013**; b) B. Metz, H. Stoll, M. Dolg, *J. Chem. Phys.* **2000**, *113*, 2563-2569.
- [24] a) J. Manson, C. E. Webster, L. M. Pérez, M. B. Hall, http://www.chem.tamu.edu/jimp2/index.html; b) M. B. Hall, R. F. Fenske, *Inorg. Chem.* 1972, 11, 768-775; c) B. E. Bursten, J. R. Jensen, R. F. Fenske, *J. Chem. Phys.* 1978, 68, 3320-3321.

Ying-Hao Lo, François P. Gabbaï

Page No. – Page No.

Cyclometalated iridium bipyridine complexes with peripheral antimony substituents